

The drift chamber project for the Super Charm-Tau Factory detector

**I. Yu. Basok,^a V. S. Bobrovnikov,^a A. V. Bykov,^a D. A. Kyshtymov,^{a,b,*}
V. G. Prisekin^a and K. Yu. Todyshev^{a,b}**

^a*Budker Institute of Nuclear Physics, 11, Akademika Lavrentieva Prospect, Novosibirsk, Russia*

^b*Novosibirsk State University, 2, Pirogova Street, Novosibirsk, 630090, Russia*

E-mail: D.A.Kyshtymov@inp.nsk.su

The Budker Institute of Nuclear Physics is actively developing a drift chamber project with a small hexagonal cell for the Super Charm-Tau Factory. A Monte-Carlo simulation of pions flight through detector has been done to estimate the drift chamber momentum resolution. To evaluate the spatial resolution of the drift chamber a small prototype has been developed. The spatial resolution measurements have been performed using cosmic particles. This experiment is carried out for He/C_3H_8 (60/40) and He/C_2H_6 (50/50) gas mixtures at different gas gains. The obtained average spatial resolution for both mixtures is less than $100 \mu\text{m}$ for gains greater than $5 \cdot 10^4$.

*6th International Conference on Technology and Instrumentation in Particle Physics (TIPP2023)
4 - 8 Sep 2023
Cape Town, Western Cape, South Africa*

*Speaker

1. Introduction

A new project of lepton collider, the Super Charm-Tau Factory (SCTF), is being evolved by the Budker Institute of Nuclear Physics. This facility will have a record luminosity of about $10^{35} \frac{1}{\text{cm}^2 \cdot \text{s}}$ in the energy range from 2 to 5 GeV. The detector Conceptual Design Report and physical program for the SCTF can be found in [1].

A new universal detector for this collider is being developed. It has to have good characteristics for measuring the coordinates, momentum and energy of particles for their subsequent identification under high luminosity conditions. One of the key parts of the new system is a drift chamber (DC). The DC is a track detector consisting of a wire structure formed by cathode and anode wires and a gas mixture. The main tasks of the drift chamber are: reconstruction of charged particles tracks, determination of their momentum and identification of the particles type by ionization energy losses.

One of the most important parameter of the DC is a momentum resolution which depends on a spatial resolution. Typically, the average spatial resolution for such facilities is more than 100 μm [2–6], but in the DC for SCTF, a better resolution can be achieved due to selected wire structure and $\text{He}/\text{C}_3\text{H}_8$ 60/40 gas mixture. In order to estimate the real value of the DC resolution a small prototype has been developed.

2. The drift chamber for Super Charm-Tau Factory

In the current project, the DC is made from carbon fiber reinforced by a plastic material. The wire structure is based on a small hexagonal cell. This shape was chosen because of advantage in a more cylindrically symmetric electric field that leads to a more circular isochrones. The length of the DC is 2000 mm, the radius of the inner cylinder is about 200 mm, the outer one is 800 mm. The total number of cell layers is 41, which are divided into 10 super layers. The average cell radius is about 7 mm.

The pion flight through DC has been simulated to estimate the DC parameters. The momentum resolution is shown in Figure 1. For pions with 1 GeV energy the resolution is equal to 0.35%.

The dE/dx resolution is about 7%. It has been estimated from CLEO-III results.

The full description of DC design has been discussed in [7].

3. The small prototype of the Super Charm-Tau Factory drift chamber

The small prototype of the drift chamber consists of a tube with a diameter of 70 mm and a length of 300 mm and two scintillation counters located on the top and bottom of the prototype. These counters form a trigger system. The top counter has a width of 50 mm and the bottom one is 100 mm. Both are 300 mm long and 10 mm thick. The tube contains 24 cathode and 7 anode wires, which form 7 hexagonal cells (see Figure 2).

High voltage is applied to the anode wires, and its value sets the required gas gain.

The drift times are measured between the signal from counters and the signal from the anode wires using the time-to-digital converter. The experiment of the spatial resolution measurements is performed using cosmic particles.

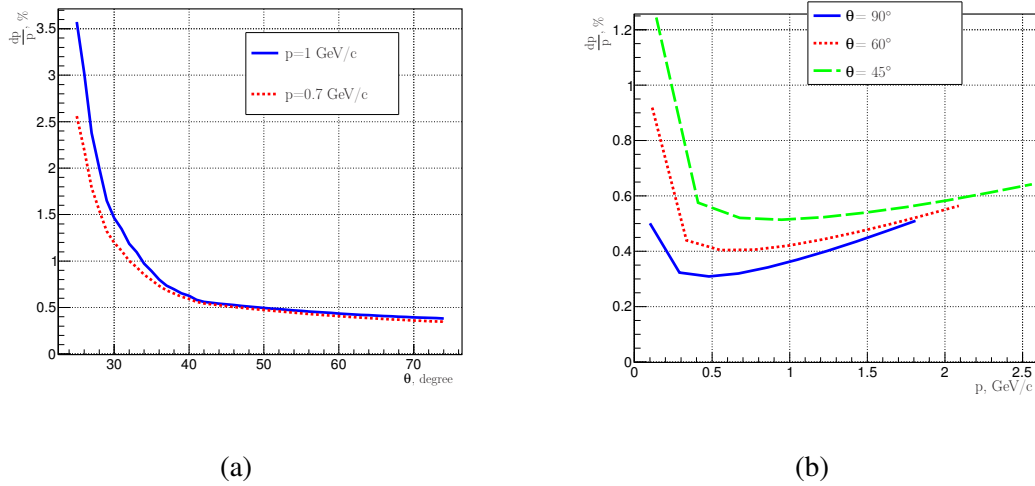


Figure 1: (a) Momentum resolution as a function of the polar angle and (b) Momentum resolution as a function of the full momentum. These figures were taken from the [7].

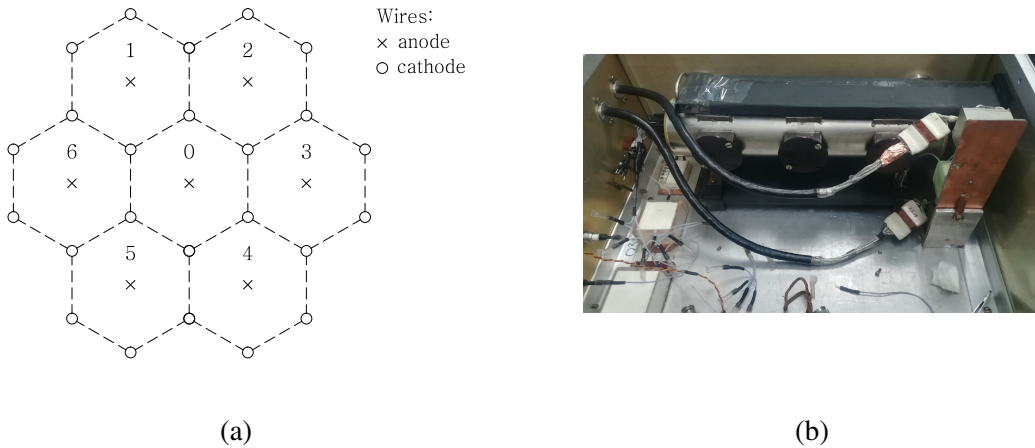


Figure 2: (a) Cell structure of the prototype and (b) The prototype photo. These figures were taken from the [8].

4. The spatial resolution measurements

There are two similar gas mixtures that can be used for SCTF purposes due to their gas properties: He/C_3H_8 (60/40) and He/C_2H_6 (50/50) (see Table 1). For these mixtures the measurements of the spatial resolution are carried out at different gas gains.

A drift time spectrum in He/C_3H_8 (60/40) mixture for the central cell is shown in Figure 3(a). The dashed line is an approximation by a piecewise linear function used to find the beginning of the spectrum.

Below are the results for He/C_3H_8 (60/40) at a gain of $7 \cdot 10^4$ for the central cell.

Gas mixtures	Ratio	Radiation Length [m]	N_p [cm^{-1}]	$E = 1 \text{ kV/cm}$		Exp.
				v [$\text{cm}/\mu\text{s}$]	$D_{ }$ [$\frac{\mu\text{m}}{\sqrt{\text{cm}}}$]	
$\text{He}/\text{C}_3\text{H}_8$	60/40	569	31	3.06	133	CLEO III BES III
$\text{He}/\text{C}_2\text{H}_6$	50/50	686	22.9	3.52	142	BELLE BELLE II

Table 1: Gas mixture properties. Here N_p is a number of electron-ion pairs per unit length, v is a drift velocity, $D_{||}$ is a longitudinal diffusion component. Parameters v and $D_{||}$ were calculated at a pressure of 1.03 atm, a temperature of 308 K and zero magnetic field.

To calibrate the $R(t)$ an algorithm using the iteration method has been developed and applied. In Figure 3(b) the $R(t)$ in five iterations are shown.

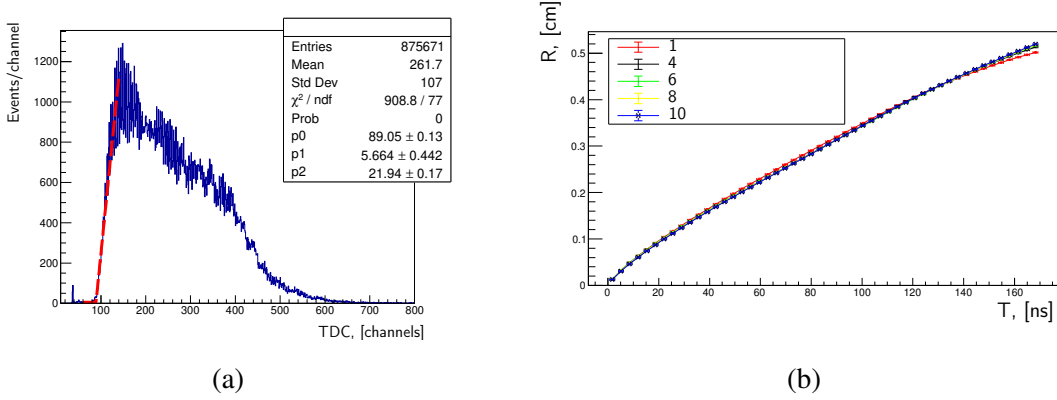


Figure 3: (a) The typical drift time spectrum and (b) The $R(t)$ dependence in the five iterations of the calibration algorithm. These figures were taken from the [8]

A comparison of simulated and experimental spatial resolutions are presented in Figure 4(a). The simulation does not take into account the constant component associated with noises, pressure and temperature fluctuations. The line shows the fit by the function:

$$\sigma(r) = \sqrt{\left(\frac{p_0}{r + p_1}\right)^{p_2} + (p_3 \sqrt{r})^2 + (p_4 e^{r p_5})^2 + p_6^2}, \quad (1)$$

where p_0, \dots, p_6 are free parameters. This function takes into account the cluster effect, diffusion component, edge effects and constant component in the resolution. The constant component has been found from comparison of simulated and experimental data. A similar parametrization of resolution was used in [9].

The cell-average spatial resolutions for two gas mixtures are shown in Figure 4(b). For gas gains of $5 \cdot 10^4$ and above, the average resolution value for both mixtures is less than $100 \mu\text{m}$.

In Table 2 the spatial resolution results are presented for each gas gain.

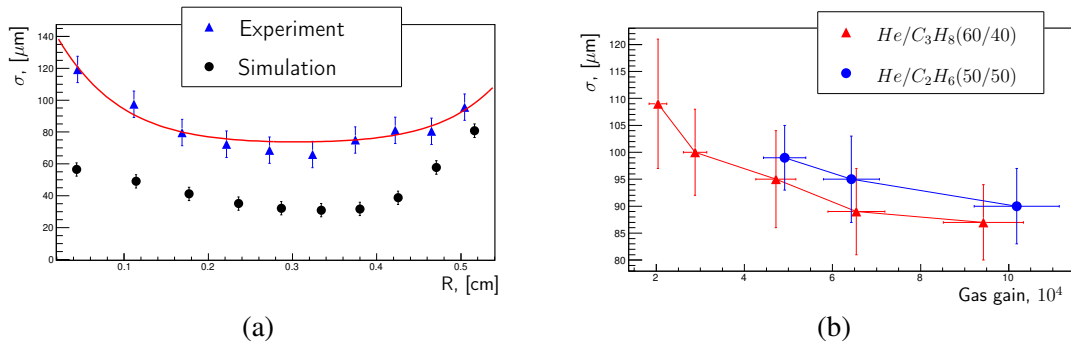


Figure 4: (a) The simulated and experimental spatial resolutions and (b) The average spatial resolutions for $\text{He}/\text{C}_3\text{H}_8$ (60/40) and $\text{He}/\text{C}_2\text{H}_6$ (50/50) gas mixtures. These figures were taken from the [8]

	$\text{He}/\text{C}_3\text{H}_8$ (60/40)	$\text{He}/\text{C}_2\text{H}_6$ (50/50)
Gas gain	$\bar{\sigma}$, μm	$\bar{\sigma}$, μm
$2 \cdot 10^4$	109 ± 12	—
$3 \cdot 10^4$	100 ± 8	—
$5 \cdot 10^4$	95 ± 9	99 ± 6
$7 \cdot 10^4$	89 ± 8	95 ± 8
10^5	87 ± 7	90 ± 7

Table 2: The measured cell-average spatial resolutions for $\text{He}/\text{C}_3\text{H}_8$ (60/40) and $\text{He}/\text{C}_2\text{H}_6$ (50/50) gas mixtures.

5. Summary

During this study the spatial resolution measurements have been carried out in $\text{He}/\text{C}_3\text{H}_8$ (60/40) and $\text{He}/\text{C}_2\text{H}_6$ (50/50) gas mixtures. An iterative process has been used to calibrate the $R(t)$ dependence. The average spatial resolution for both gas mixtures is better than $100 \mu\text{m}$ for gas gains above $5 \cdot 10^4$.

The results of this study show that it is possible to achieve good measurement accuracy in a drift chamber with the small hexagonal cells.

6. Acknowledgments

This study was conducted within the scientific program of the National Center for Physics and Mathematics, section #6. Stage 2023-2025.

References

- [1] The Super Charm-Tau Factory. *Conceptual Design Report*, <https://ctd.inp.nsk.su/c-tau/>
- [2] D. Peterson et. al, *The CLEO III drift chamber*, Nucl. Instr. and Meth. Res. A 478 (2002) 142-146, [https://doi.org/10.1016/S0168-9002\(01\)01737-5](https://doi.org/10.1016/S0168-9002(01)01737-5).

- [3] G. Sciolla et al., *The BaBar Drift Chamber*, Nucl. Instr. and Meth. Res. A 419 (1998) 310-314, [https://doi.org/10.1016/S0168-9002\(98\)00804-3](https://doi.org/10.1016/S0168-9002(98)00804-3).
- [4] M. Ablikim et al., *Design and Construction of the BES III Detector*, Nucl. Instr. and Meth. Res. A 614 (2010) 345-399, <https://doi.org/10.1016/j.nima.2009.12.050>.
- [5] S. Uno, *The Belle central drift chamber*, Nucl. Instr. and Meth. Res. A 379 (1996) 421-423, [https://doi.org/10.1016/0168-9002\(96\)00555-4](https://doi.org/10.1016/0168-9002(96)00555-4).
- [6] T. Abe et al., *Belle II Technical Design Report*, arXiv preprint arXiv:1011.0352 (2010), <https://doi.org/10.48550/arXiv.1011.0352>.
- [7] I. Yu Basok, et al., *The drift chamber project for the Super Charm-Tau Factory detector*, Nucl. Instr. and Meth. Res. A 1009 (2021) 165490, <https://doi.org/10.1016/j.nima.2021.165490>.
- [8] I. Yu Basok, et al., *The spatial resolution measurements on the small prototype of the Super Charm-Tau Factory drift chamber*, Nucl. Instr. and Meth. Res. A 1064 (2024) 169419, <https://doi.org/10.1016/j.nima.2024.169419>.
- [9] T. V. Dong et al., *Calibration and alignment of the Belle II central drift chamber*, Nucl. Instr. and Meth. Res. A 930 (2019) 132-141, <https://doi.org/10.1016/j.nima.2019.03.072>.